Chemical Engineering Journal 463 (2023) 142245

Contents lists available at ScienceDirect

Chemical Engineering Journal

journal homepage: www.elsevier.com/locate/cej

Lignin valorization in thermoplastic biomaterials: from reactive melt processing to recyclable and biodegradable packaging

Angelica Avella [a,b], Marcus Ruda [c], Claudio Gioia [d], Valentina Sessini [a,b,e], Thomas Roulin [c], Christopher Carrick [c], Johan Verendel [c], Giada Lo Re [a,b,*]

[a] Department of Industrial and Materials Science, Chalmers University of Technology, Rännvägen 2A, 41258 Gothenburg, Sweden
[b] Wallenberg Wood Science Centre, Chalmers University of Technology, Kemigården 4, 41258 Gothenburg, Sweden
[c] Lignin Industries AB, Rubanksgatan 9, 74171 Knivsta, Sweden
[d] Department of Physics, University of Trento, via Sommarive 14, 38123 Povo (TN), Italy
[e] Department of Organic and Inorganic Chemistry, Institute of Chemical Research "Andrés M. del Río" (IQAR), Universidad de Alcalá, Campus Universitario, 28871 Alcalá de Henares, Madrid, Spain

1. Introduction

Despite the growing awareness of the risks of plastic pollution, more than 99 wt% of globally produced plastics are still non-biodegradable and are derived from fossil fuels [1]. Around 60 wt% of all the plastics ever produced has been deposited in nature or accumulated in landfills, with a risk to life and ecosystems [2]. Currently, more than 40 wt% of non-biodegradable plastics is used in packaging, despite the short service time typical for such materials [2].

Different strategies can be devised to reduce the environmental impact of short-life single-use items and increase resource efficiency by, for example, re-designing their processes with sustainable methods and focusing on biodegradables [3].

Lignin is an attractive renewable resource since it is one of the most abundant natural polymers on Earth and the main by-product of the pulp and paper industry, representing 15 – 35 wt% of lignocellulosic biomass [4]. Lignin is produced in plants by photosynthesis (consuming carbon dioxide) and the polymerization of carbohydrates [5]. It undergoes degradation by fungi [5], but only when other easily available carbon sources are present [6]. In aerobic microbial composting, lignin is the most recalcitrant structure among the wood components [7]. Between 50 and 60 million tons of industrial lignin are generated every year by the pulp and paper industry, the majority of which (98 %) is exploited as a low-cost biofuel [8]. In addition to the economic advantage of its large availability, its renewability, biodegradability and an attractive chemical structure, make the exploitation of industrial lignin of interest in biosourced and biodegradable materials [9].

Recently, considerable effort has been devoted to blending lignin with other biodegradable thermoplastic polymers to produce biomaterials with interesting properties [10]. However, poor interactions at the interface with polymer matrices hinder the desired reinforcement even at low lignin contents [11,12]. Moreover, the brittleness and high glass transition temperature of industrial lignin limit the amount of lignin that can be loaded and its melt processing [13], requiring the use of plasticizers [14] and compatibilizers [15]. Further complications arise because the lignin has an extremely heterogeneous structure due to differences in the biomass sources and extraction methods. Organic solvent-based procedures for purification and fractionation are often employed to obtain a more homogeneous and defined lignin [16], but this reduces the sustainable and economic advantages of using industrial lignin.

The various functional groups in lignin offer several possibilities for its chemical derivatization. Prior to melt processing, lignin has been modified by *e.g.* lowering its glass transition temperature and/or its melt viscosity [17]. These strategies resulted in improved interaction with polymer matrices [10,18], allowing lignin incorporation up to 70 wt% [19,20], and exceptionally to 95 wt% [21], but dramatically reducing the deformability and requiring high processing temperature. With a few exceptions [20,22], lignin modification has been performed in organic solvents [19,21,23–27], followed by purification steps. The complexity and heterogeneity of the lignin structure complicate its characterization, limiting the reproducibility and scalability of the processes [28,29].

Reactive extrusion (REx) is a scalable and sustainable alternative to solvent-based modification, making single-step continuous chemical reactions possible during processing [30]. While compounding in a twin-screw extruder, which ensures an efficient mixing and extrusion of heterogenous compounds, it is possible to carry out chemical reactions.

* Corresponding author.
E-mail addresses: avella@chalmers.se (A. Avella), marcus.ruda@lignin.se (M. Ruda), claudio.gioia@unitn.it (C. Gioia), valentina.sessini@uah.es (V. Sessini), thomas.roulin@lignin.se (T. Roulin), christopher.carrick@lignin.se (C. Carrick), johan.verendel@lignin.se (J. Verendel), giadal@chalmers.se (G. Lo Re).

https://doi.org/10.1016/j.cej.2023.142245
Received 10 November 2022; Received in revised form 27 January 2023; Accepted 28 February 2023
Available online 3 March 2023

Twin-screw extruders are continuous plug flow reactors suitable for REx, in which the screws rotation provides the needed stirring for efficient mass and energy (temperature and shear) transfer [30]. Therefore, REx results as a cost-effective single-step materials modification and manufacturing, which supports their commercial viability and cost-competitiveness. This method has been explored for various chemical reactions such as polymerization [31], grafting [32], branching and functionalization [30].

REx has been exploited to achieve compatibilization of lignin with thermoplastic matrices through the use of coupling agents [33], cross-linkers [12,34,35] or functionalized matrices [36,37]. To our knowledge, only a few studies have reported the modification of lignin via REx, but the reported strategies required pre- and/or post-purification steps and the use of organic solvents. Bridson et al. [38] have described the succinylation of different types of lignin via REx, studying different extraction methods and emphasizing the need for a purification step for a successful reaction. Milotskyi et al. [39] have esterified Kraft lignin through REx with succinic and maleic anhydrides, using plasticizers (greater than15 wt%) because of the poor melt processability of lignin, and including post-extrusion purification steps. Farhat et al. [40] prepared lignin-based hydrogels for drug delivery through REx with citric acid that served both as plasticizer and crosslinker. Their results indicate the need of at least 60 wt% of citric acid to extrude lignin, while Li et al. [41] produced vinyl silylated lignin via REx as a precursor for a two-step polyacrylonitrile/lignin copolymerization in dimethyl sulfoxide. All these studies did not demonstrate the use of modified lignin in thermoplastic biomaterials.

Designing biomaterials from the molecular engineering to the easy melt processes and sustainable end-of-life options, the present work demonstrates a circular route for upgrading lignin to meet the demand for industrially scalable thermoplastic alternatives to non-degradable fossil-based plastics. Our REx process for the modification of unrefined lignin requires neither pre- nor post-purification steps, nor does it use organic solvents or plasticizers. The inherent sustainability of the process therefore facilitates the industrial scale-up. Moreover, considering the importance of packaging in the market, we have targeted the production of film-blowable biomaterials that can become sustainable alternatives to oil-based products [42]. We have selected poly(butylene adipate-co-terephthalate) (PBAT) as matrix, which is an increasingly popular biodegradable polyester on the market [43] with mechanical properties similar to those of low-density polyethylene and good melt processability [44]. Our hypothesis was that PBAT would support lignin biodegradation, as more readily available carbon source [6]. The incorporation of industrial lignin in PBAT involves a sustainable synergy in which PBAT facilitates film blowing with a high lignin content, while lignin increases the bio-content and decreases the carbon footprint of PBAT. The study develops an unprecedented sustainable pathway starting from a by-product of the Kraft process up to the industrial scale manufacture of a commercial product. Matching the European requirements and limitations related to single-use plastics and plastic packaging [45,46], we believe that the demonstrated mechanical recyclability and disintegration under composting conditions of the biomaterials fulfil the most sustainable end-of-life options.

2. Materials and methods

2.1. Materials

Lignin extracted from softwood biomass by the Kraft pulping process and by the LignoBoost recovery method (Stora Enso, Sunila, Finland) was used as received. The ultimate and proximate analyses of this lignin are provided elsewhere [47]. It has a glass transition temperature (T_g) of 155 °C, a molecular weight (M_w) of 3300 g/mol and a Polydispersity Index (PDI) of 2.3. Poly(butylene adipate-co-terephthalate) (PBAT) was purchased from Jinhui ZhaoLong High Technology Co. Ltd (P.R. China), with a declared density of 1.26 g/cm^3 and a melt flow rate $\leq$ 5 g/10 min (ISO 1133) at 190 °C and 2.16 kg. Formic acid, methyl oleate, and H_2O_2 (35 %) were purchased from Alfa Aesar (Germany). Na_2SO_4, dimethyl sulfoxide (DMSO), $CDCl_3$, dimethyl amino pyridine, guaiacol, butyric acid, ethyl acetate, HCl and magnesium sulphate were purchased from Sigma Aldrich AB (Sweden) and used as received.

2.2. Methods

2.2.1. Methyl oleate oxidation (methyl 9,10-epoxystearate)

Methyl 9,10-epoxystearate (eOil) was synthesized from methyl oleate according to the following procedure. 6 kg (20,24 mol) of methyl oleate were mixed with 600 ml (10,68 mol) of formic acid and heated to 70 °C. The heater was turned off and 191 ml (22,26 mol) of H_2O_2 was added slowly to maintain a temperature of ca. 75 °C. After the addition of H_2O_2, the heater was set to 70 °C and the reaction was followed by Nuclear Magnetic Resonance (NMR). When the reaction was complete, the heater was turned off with maintained stirring and 2L of water was added to stop the reaction and remove the formic acid. The reaction products were extracted 5 × 2L of water. The water was removed, and the oil was dried with 200 g of Na_2SO_4 overnight. The Na_2SO_4 was then removed by filtration. The reaction yield was 93.4 %.

2.2.2. Synthesis of Renol

Renol was synthesized by reactive extrusion after manual premixing of lignin with methyl 9,10-epoxystearate (eOil) (Fig. 1). The REx was carried out in a single-screw extruder (Brabender GmbH & Co., Germany) with a temperature profile of 120–160-150–150 °C (feeder to die) and 60 rpm with a round hole die (3 mm in diameter and 26.7 mm in length) and a barrier screw (compression ratio 2.5:1, diameter D of 19 mm and length of 25D) equipped with a mixing element. The residence time was ca. 15 min.

The temperature profile for REx was selected to reach as fast as possible the temperature of 160 °C, to increase the reaction kinetics and to overcome lignin glass transition temperature to enhance the lignin mobility. Then the temperature was lowered to 150 °C to keep the reaction progresses and complete at a suitable melt viscosity, which ensures a good mixing, and avoid a possible thermomechanical degradation. This temperature profile was chosen after several tests for which lower temperatures did not allow for a full mixing of the components and for the reaction completion between the oil and the lignin, while higher temperatures resulted in significant discoloration and visible degradation and evident release of volatiles with foaming (Figure S1).

Three different amounts of eOil (7, 12 and 25 wt%) were tested and the 12 wt% was selected as the optimal amount for further experiments, according to the glass transition temperature achieved (T_g 123, 112 and 82 °C respectively) (Fig. 2b).

2.2.3. Biomaterials preparation

Different amounts of Renol between 0 and 90 wt% (Table 1) were premixed with PBAT pellets and melt processed in an internal mixer AEV 330 (50 cm^3) (Brabender GmbH & Co., Germany) at 165 °C and 60 rpm for 15 min. Three reference materials were produced under the same conditions by mixing PBAT with 35 wt% pristine lignin (35L-P) and with 35 wt% pristine lignin and 5 wt% methyl oleate (35L-5O-P) or methyl 9,10-epoxystearate (35L-5eO-P). 35 wt% lignin and 5 wt% are the equivalent lignin and methyl oleate amounts, respectively, present in 40 wt% Renol, selected as the target composition. For further testing, PBAT and the processed biomaterials and references were formed into 1 mm thick square films by compression molding (Buscher-Guyer KHL 100, Switzerland) at 120 °C, at 40 bar for 3 min and at 500 bar for 1 min.

2.2.4. Film blowing

Prior to film blowing, PBAT and biomaterials with 10, 30 and 40 wt% Renol were melt extruded in the single-screw extruder at 40 rpm with a temperature profile of 120–160-140–130 °C (feeder to die) using the

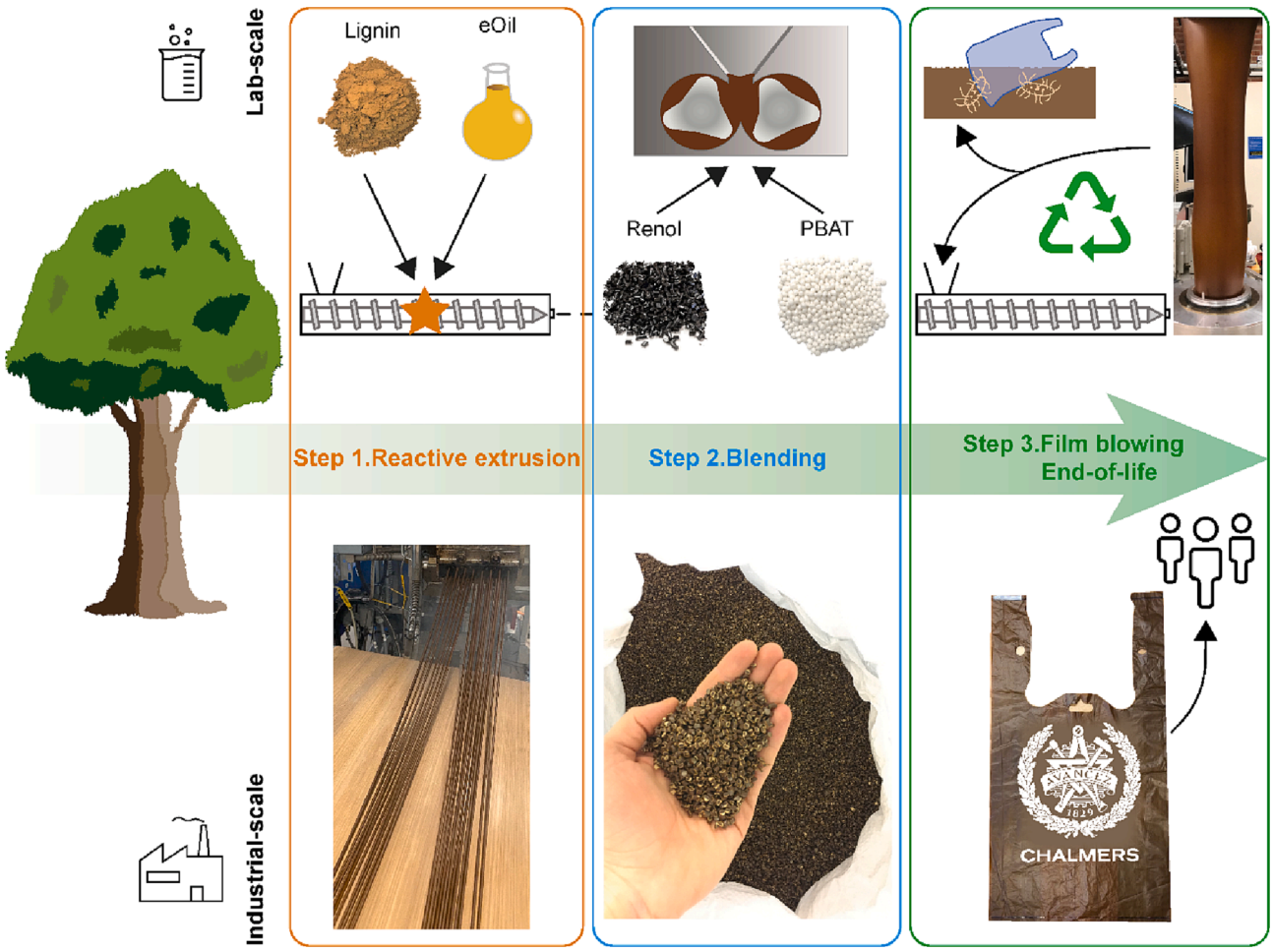

Fig. 1. Scheme of the multistep strategy developed: Step 1. Reactive extrusion of lignin with methyl 9,10-epoxystearate to produce Renol; Step 2. Melt processing of Renol with PBAT in an internal mixer; Step 3. Film blowing of Renol/PBAT blends and their recycling. Industrial scale corresponding steps for the production of the biomaterials and a sample of a shopping bag (bottom side). The bag was produced at an industrial facility operating at a production rate of 50 kg/h and film-blown with a die temperature of 160 °C.

same screw and die as Renol REx. The extruded strands were pelletized and re-extruded at 20 rpm with a temperature profile of 120–160-150–120 °C (feeder to die) through a film blowing die with cooling ring. The blown films were collected and pulled by rotating rolls at the top of the die.

2.2.5. *Mechanical recycling*

The blown films of PBAT and 40R-P were stored in sealed plastic bags for one year under ambient conditions. They were manually cut and reprocessed in the internal mixer, followed by compression molding, with the same processing parameters as those used for the biomaterials preparation.

2.2.6. *Characterization methods*

Various techniques were used to characterize are described in the Supporting Information (SI, Ch.2).

3. Results and discussion

A laboratory-scale procedure for the modification of lignin via reactive extrusion (Step 1, Fig. 1), followed by its blending with a biodegradable polyester (PBAT) (Step 2, Fig. 1) to produce filmable biomaterials has been designed and two end-of-life options were evaluated (Step 3, Fig. 1). The Renol reactive extrusion and blending with PBAT have been upgraded to an industrial scale, including the production of shopping bags as proof-of-concept for sustainable packaging (Bottom of Fig. 1).

3.1. *Step 1: Reactive extrusion of thermoplastic lignin (Renol)*

Lignin plasticization was achieved by the reactive extrusion of industrial Kraft lignin with bio-sourced methyl 9,10-epoxystearate (Fig. 2a), during which the lignin powder was transformed into a dark brittle solid. At a high temperature, the constrained oxirane ring easily reacts with nucleophilic moieties such as phenols, aliphatic alcohols and carboxylate groups, undergoing ring-opening [48],and leading to the formation of a new ether or ester bond, and a new hydroxyl group. It is worth to note that the results commented refer to the suitable temperature profile selected (120–160-150–150 °C, details in Section 2.2.2) after investigation of REx at different temperatures for the sake of completion of the reaction while avoiding degradation during the extrusion time. Three different amounts of eOil (7, 12 and 25 wt%) were tested and the glass transitions of the products were found to be $T_g \sim$ 123, 112 and 82 °C respectively. No melting of the eOil (melting temperature = 7 °C) was observed in the Renol curves, indicating that the epoxy moieties were completely grafted onto the lignin (Fig. 2b). REx with 12 wt% eOil reduced the lignin glass transition temperature by ca. 40 °C, confirming the successful modification of the lignin structure and an increase in its macromolecular mobility sufficient to provide a suitable thermoplastic character. Considering the full reaction of eOil from

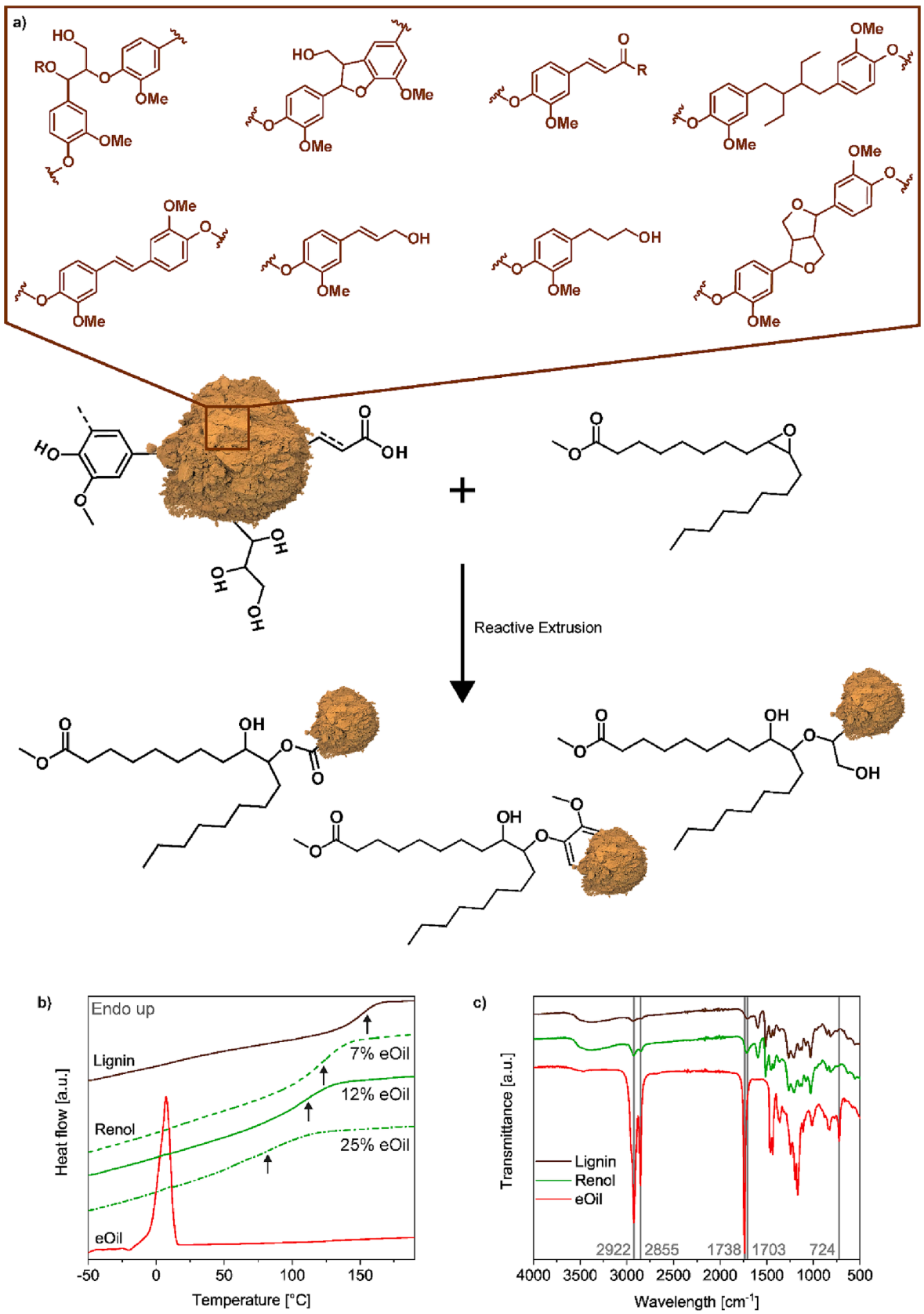

Fig. 2. A) Proposed reaction scheme between lignin functionalities and eOil during extrusion. Inset with typical lignin functional groups at the top. b) Second heating differential scanning calorimetry thermograms of lignin, eOil and Renol reacted with 7, 12 and 25 wt% of eOil. The lignin glass transition temperature, indicated with an arrow, is gradually shifted towards lower temperatures with increasing eOil wt.%. c) Spectra from Fourier-transform infrared spectroscopy in transmission mode of Renol and its components (lignin and eOil). The vertical lines show the peaks that indicate changes due to the reaction.

Table 1
Compositions in weight percentages of the materials produced. The raw lignin and eOil equivalent contents are based on the Renol composition (88:12 lignin: eOil).

Material	PBAT [wt%]	Renol [wt%]	Equivalent lignin content [wt%]	Equivalent eOil content [wt%]
Lignin (L)	–	–	100	–
Renol (R)	–	100	88	12
PBAT (P)	100	–	–	–
10R-P	90	10	≈ 9	≈ 1
30R-P	70	30	≈ 26	≈ 4
35L-P	65	–	35	–
35L-5O-P*	60	–	35	–
35L-5eO-P	60	–	35	5
40R-P	60	40	≈ 35	≈ 5
50R-P	50	50	≈ 44	≈ 6
70R-P	30	70	≈ 62	≈ 8
90R-P	10	90	≈ 79	≈ 11

*The reference 35L-5O-P was produced using 35 wt% lignin and 5 wt% methyl oleate. The methyl oleate is the non-epoxidized structure of methyl 9,10-epoxystearate (eOil).

differential scanning calorimetry (DSC), 12 wt% theoretically corresponds to 67 mol.% of lignin macromolecules grafted with one eOil chain (assuming eOil number average molecular weight (M_n) = 312.5 g/mol and lignin M_n = 1435 g/mol). A higher eOil content led to a greater plasticization of the lignin and reduced its reinforcing effect. This composition was preferred, and it was further characterized by structural analyses, to investigate the reaction mechanism and the resulting lignin structural changes.

According to the size exclusion chromatography in dimethyl sulfoxide (Figure S2), REx led to a substantial increment in both the molecular weight and the polydispersity of the lignin resulting in Renol with M_w = 12000 g/mol and PDI = 5.2 (neat lignin M_w = 3300 g/mol; PDI = 2.3). These increases may indicate a concomitant oligomerization and condensation of lignin macromolecules under temperature and shear stresses during REx.

Fourier-Transform Infrared Spectroscopy (FTIR) was performed to assess the chemical grafting of eOil on lignin and to confirm its complete conversion. Fig. 2c shows the FTIR spectra of Renol, neat lignin and eOil. In the Renol spectrum the main signals of the neat lignin are visible [39,49]. The increase in the signals at 2922 and 2855 cm^{-1}, commonly associated to the CH_2 stretching, suggests the presence of the aliphatic fatty acid structure. The absence of the signal at 724 cm^{-1}, typically related to oxirane moieties, indicates that the epoxy ring has been completely consumed during REx, consistent with the lack of eOil melting found in the DSC analysis. The eOil signal at 1738 cm^{-1}, related to the methyl ester group, seems to contribute to a sharpening of the lignin ester signal of Renol at 1703 cm^{-1}.

The extent of the chemical modification was further investigated by combining ^{31}P NMR and 2D-Heteronuclear Single Quantum Coherence (HSQC) to characterize the detailed lignin structure and this provided confirmation that the epoxidized fatty acid methyl ester had been successfully grafted (Figure S3 and S4). ^{31}P NMR provides valuable information regarding the most frequently recurring functional groups of lignin [49,50] (*i.e.* phenols, aliphatic alcohols and carboxylic acids) while the 2D-HSQC analysis yields an overview of the main connecting units and functionalities involved in the lignin backbone (Fig. 3).

As shown in Table 2, the ^{31}P NMR analysis confirmed that there was a substantial percentage reduction of 33.3 % in the carboxylic acid content and a mild reduction in the contents of aliphatic alcohols and phenols (19 and 8.2 %, respectively). The carboxylic acid content was expected to decrease as a result of the grafting of eOil on lignin, but the reduction in the content of aliphatic alcohols was unexpected, since the creation of each new alcoholic moiety is associated with the opening of an oxirane ring. This is related to the undesired processes able to consume aliphatic hydroxyls such as the subsequent hydroxyl/epoxy or dehydration reactions occurring under REx. The number of phenol groups was however only marginally affected, suggesting that their reactivity is poor under the conditions adopted. The slight increase in the amount of condensed phenols (5–5, 4O5 and $\beta5_2$) from 43 to 45 %, could be the result of condensation reactions at the high processing temperature [38,39].

The HSQC spectra reported in Fig. 4 make it possible to qualitatively analyze and compare the main structural features of the Kraft lignin and of the Renol. The structure of the neat lignin (after the Kraft process) differs significantly from the native structure (Figure S5 and Table S1) [49,51–55]. Connecting units such as β5 (86.9/5.40 ppm), $\beta\beta_1$ (85.1/4.61 ppm, 53.5/3.04 ppm and 71.1/3.81–4.15), $\beta\beta_2$ (33.5/2.42–2.53 and 42.8/1.86) and stilbene (129.0/7.30–6.96 ppm), appear to dominate, whereas the βO4 (59.4/3.42–3.71 ppm, 71.4/4.71 ppm and 83.5/4.27 ppm), even when connected to residual carbohydrates (82.0/4.77 ppm), was greatly reduced. Common end-groups in lignin are detected at 120.9/5.34 ppm for cinnamyl alcohol (CA), at 31.1/2.48 ppm and 34.4/1.66 ppm for dihydro coniferyl (DCA) alcohol and at 124.0/7.78–7.45 ppm for conjugated acids and carbonyls (CC). The region related to aliphatic sidechains includes signals detectable at 30–10/2.5–0.5 ppm, while unsaturated structures appear at 130–115/57–5.2 ppm.

Fig. 4 shows that the Renol spectrum confirms that connecting units such as $\beta\beta_1$, $\beta\beta_2$, $\beta5_1$ and stilbene units survived the REx conditions [49,51–55]. Although $\beta O4_1$ units appear to be preserved, no signals related to $\beta O4_2$ (82.0/4.77 ppm) and to all the carbohydrate residues (76–72/3.5–3.0 ppm) [49,51–55] were detected after REx, indicating that their thermal stability was poor. The HSQC analysis of terminal groups in Renol shows the presence of aliphatic alcohols such as cinnamyl and dihydro coniferyl alcohols, but the signals related to the conjugated carboxylic acids (124.0/7.78–7.45 ppm) [49,51–55] completely disappeared, indicating their preferential reactivity towards epoxy groups. Finally, the increase in the sharp signal at 128/5.3 ppm in the unsaturated region suggests that new double bonds have been produced as a result of undesired dehydration processes, which may also be responsible for the decrease in the number of alcoholic groups detected by ^{31}P NMR.

The grafting of eOil onto the lignin backbone in Renol is indicated by several new signals in the aliphatic region. The fatty acid aliphatic chain shows $–CH_2$- signals at 20–40/1.2–1.7 ppm, at 42.1/2.4 ppm, 33.8/2.3 ppm and 27.3/2.0 ppm while the terminal methyl group appears at 14.4/0.87 ppm. The methoxy group gives a sharp signal at 51.6/3.6 ppm. A comparison between the integral of the $–CH_2$- signals to the $–CH_3$ signal at 14.4/0.87 ppm suggests that there was no significant occurrence of transesterification reactions. The creation of new chemical bonds anchoring the methyl 9,10-epoxystearate is indicated by the absence of the signals associated with the oxirane ring (57.3–57.4/2.9–2.8 ppm) [56] together with a set of signals appearing at 76.9/4.7 ppm, 70.1/3.4 ppm and 73.6/3.2 ppm with sharp profiles. These results suggest that these signals are related to reacted sites on the fatty acid rather than on lignin structures. These signals were identified by comparison with those of synthetic model compounds (details in SI Ch. 3, Fig. S6, S7 and S8). The presence of ester bonds produced by the reaction between carboxylic acids and the epoxy ring is indicated by the characteristic signal at 76.9/4.7 ppm together with that of the new hydroxyl group at 70.1/3.4 ppm derived from the opening of the oxirane ring. The signal at 73.6/3.2 ppm is consistent with the ether bond obtained by the reaction of the aliphatic alcohols. The absence of signals related to aromatic ethers, otherwise detected at 82.4/4.1 and 70.2/3.5, confirmed the poor reactivity of phenols under these reaction conditions, consistent with the ^{31}P NMR results.

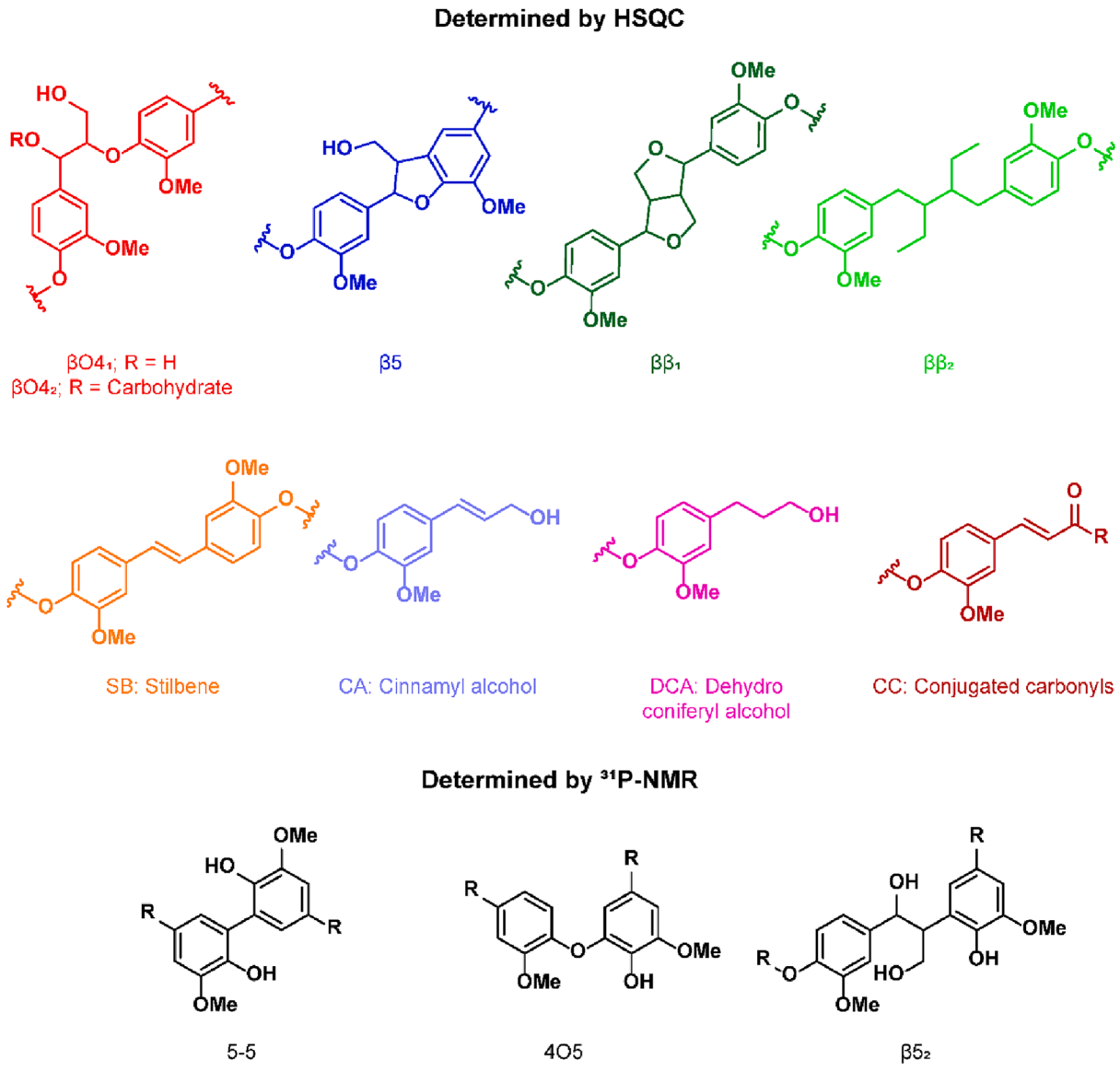

Fig. 3. Main lignin structures detected by HSQC (color code linked to Fig. 4) and ^{31}P NMR.

Table 2
Amounts of functional hydroxyl groups in lignin and Renol assessed by ^{31}P NMR and the percentage reduction after the reactive extrusion.

	Lignin	Renol	% Reduction
Aliphatic OH (mmol/g)	2.1	1.7	19.0
COOH (mmol/g)	0.6	0.4[b]	33.3
Phenols (mmol/g)	4.9	4.5[b]	8.2
Condensed Phenols (%)[a]	43	45[b]	–

[a] Calculated over the total amount of phenols.
[b] Values normalized with respect to the lignin content of the sample (88 wt%).

3.2. Step 2: blending of Renol/PBAT biomaterials

Renol, from 10 to 90 wt%, was blended with PBAT in an internal mixer (Table 1 and Fig. 5a), and the thermal properties of the biomaterials produced were studied to assess the changes in thermal transitions, crystallinity, and degradation behavior compared with those of the neat materials (Table S2). In the DSC scans (Figure S9), the PBAT glass transition gradually increased (up to 50 degrees of increment) with increasing Renol content. This reduction in PBAT chain mobility is consistent with an improved dispersion and/or a strong interaction of the rigid aromatic structure of Renol with the polyester, which also contains aromatic units. Due to the overlapping of the Renol glass transition and PBAT melting, the full miscibility of Renol and PBAT could not be further demonstrated.

The thermogravimetric analysis of the biomaterials shows that there are two main degradation steps consistent with the lignin and PBAT contents (Table S2 and Figure S10). The amount of char residue at 800 °C increased with increasing lignin content, suggesting potential flame retardant properties [57].

The mechanical properties of the biomaterials were evaluated by tensile testing at room temperature (Table S3). 10 wt% Renol shows a greater reinforcement and greater deformability than the neat PBAT, indicating that the lignin does not hinder PBAT deformability (Fig. 5b and 5c). At 40 wt% Renol, the biomaterial had the highest modulus while retaining a high deformability (≈ 550 %), and this was therefore selected as the most suitable composition for film blowing as proof of concept of the more challenging among the melt processes, which requires defect-free interfaces. (Section 3.3). It is worth to note that the tunability of the mechanical properties and easy processability allow for different shaping of the biomaterials from melt spinning to injection molding.

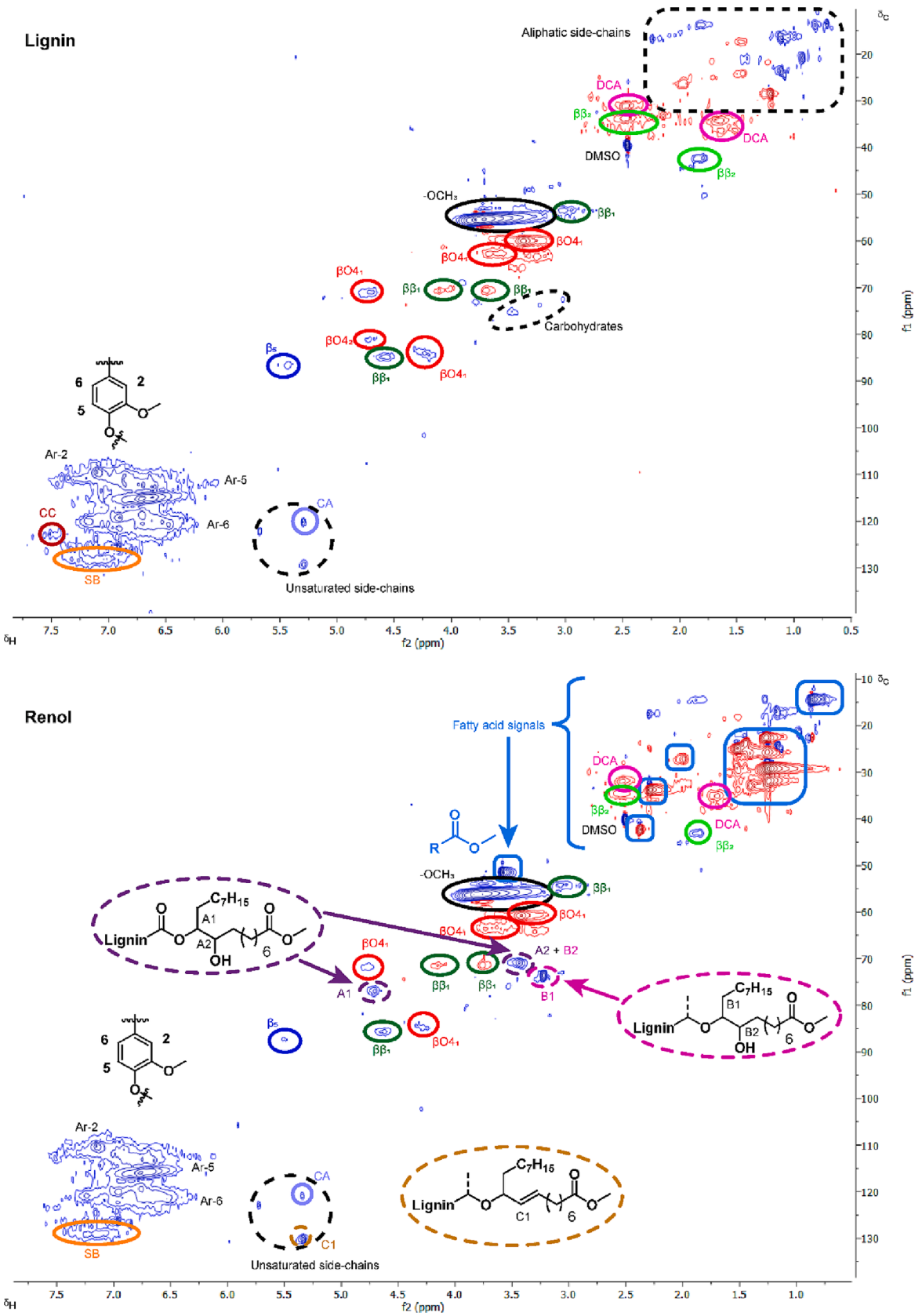

Fig. 4. 2D-HSQC analysis of neat Kraft lignin and Renol. The typical chemical structures of lignin are identified, together with the signals from eOil, and new bonds between the two components formed by REx. The encircled signal areas are color-coded according to the structures in Fig. 3.

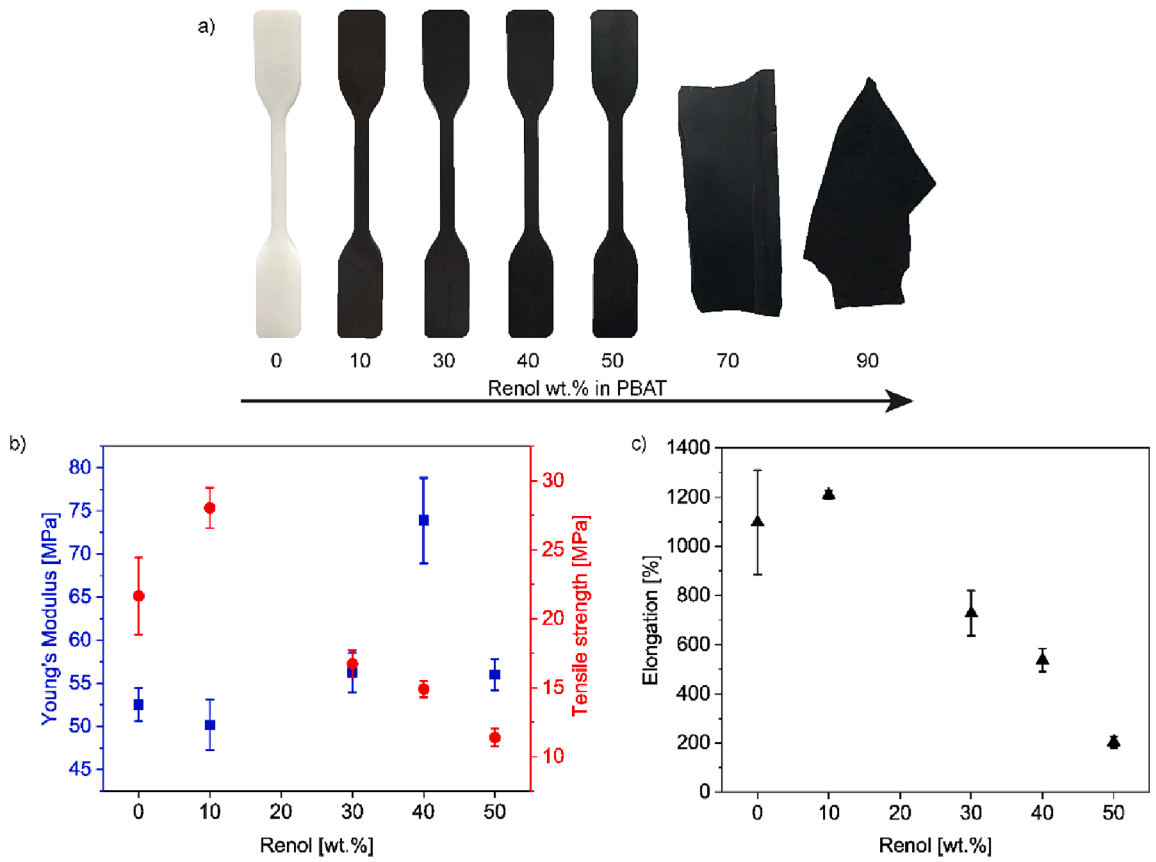

Fig. 5. a) Photographs of tensile specimens of biomaterials with different Renol contents. The biomaterials containing 70 and 90 wt% Renol were too brittle to produce specimens, and the compression molded films are therefore shown. Tensile average values with standard deviation of b) Young's modulus and tensile strength and c) elongation at break of Renol/PBAT biomaterials.

Our data were compared with published values for the melt blending of PBAT with neat and modified lignins (Fig. 6). All the reported strategies for lignin modification required the use of organic solvents, in contrast to our work. At high lignin contents (40 and 50 wt%), our strategy led to stiffness values similar to those reported by Wang et al. [22], for lignin esterified via a microwave-assisted reaction in the presence of catalysts, followed by purification in ethanol. It is unclear how the purification step affects the lignin fractionation since it is partially soluble in ethanol. We obtained the greatest elongation at break for biomaterials containing up to 30 wt% lignin. At higher contents our results are again comparable to those of Wang et al. [22] and those of Xiong et al. [37].

3.3. Step 3: Film blowing and end-of-life

As controls, neat lignin/PBAT (35L-P), neat lignin/methyl oleate/

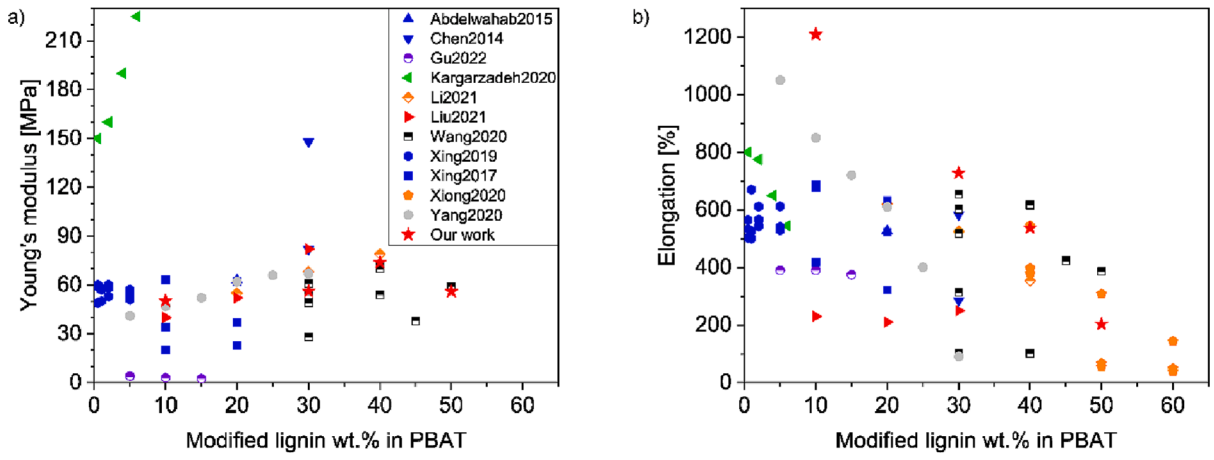

Fig. 6. A) young's modulus and b) elongation at break values of lignin/pbat blends. points with the same colour indicate materials containing the same pbat grade. the following references have been considered: abdelwahab 2015[58], Chen 2014 [16], Gu 2022 [59], Kargarzadeh 2020 [60], Li 2021 [61], Liu 2021 [24], Wang 2020 [22], Xing 2019 [25], Xing 2017 [23], Xiong 2020 [37], Yang 2020 [26]. Glasser et al. [27] have film-blown modified lignin/PBAT blends but the tensile properties were reported only as percentage changes relative to neat PBAT.

PBAT (35L-5O-P) and neat lignin/eOil/PBAT (35L-5eO-P) were blended in a single step and their properties were compared with those of 40R-P to assess the effect of REx on the feasibility of film blowing. Oil migrated to the surface of the compression-molded sheets of 35L-5eO-P and 35L-5O-P indicating the importance of grafting the oil onto the lignin by REx before blending with PBAT (Figure S11). The 40R-P sheet showed no oil phase separation, in line with the fact that there was no evidence of melting of the oil in the Renol DSC analysis. Further evidence of the better interaction between PBAT and Renol can be seen in the T_g value of 35L-5O-P, which was the same as that of neat PBAT T_g (–33 °C) (Table S2 and Figure S9). The dynamic mechanical thermal analysis (Table S4) confirmed the largest increase in T_g of 15 °C for 40R-P.

The stress–strain curves in Fig. 7a show that 40R-P had both the highest elongation at break and the highest strength, indicating that the lignin modification led to an improved interaction/dispersion. The new ester moieties formed during REx (Fig. 4) and the methyl esters of the eOil probably led to stronger interactions with PBAT. The stiffening effect of neat lignin in 35L-P can be ascribed to the higher glass transition of neat lignin than that of Renol. The elongation at break of 35L-P was half that of 40R-P, showing that a high content of lignin leads to brittleness [37], which is detrimental to film blowing. The film blowing process requires highly deformable materials with a high melt strength, enabling bubble formation and giving endurance while the molecular chains undergo radial and longitudinal orientations. Methyl oleate acted as a plasticizer in 35L-5O-P, since it reduced the reinforcement effect of lignin but still showed half the deformability of 40R-P. The reference with epoxidized oil showed a brittle behavior (elongation ≈ 20 %, Young's modulus ≈ 75 MPa), supporting the benefit of a two-step melt processing approach. The addition of PBAT (60 wt%) reduced the probability of a grafting reaction onto lignin, hindering the compatibilization at the lignin/PBAT interface.

The superior properties of 40R-P are evident in the work to fracture (Fig. 7b). Its larger elongation and greater strength resulted in a toughness more than doubled that of the other references. The two-step REx approach preserved a high level of PBAT toughness and the beneficial strengthening of a high renewable lignin content.

The study by scanning electron microscopy of 35L-P (Figure S12) revealed a debonding between the lignin aggregates and the matrix. At the same magnification, the surface of 40R-P appeared instead to be monophasic at the observed scale, without any debonding, pull-out, or lignin aggregates. This morphological feature reveals the good miscibility between Renol and PBAT, already suggested by the thermal and mechanical analyses.

Dynamic rheological analysis was carried out to assess the viscoelastic properties and melt processability of 40R-P and of the references. The frequency sweeps recorded at the processing temperature (Fig. 7c and 7d) show that the storage moduli of 40R-P are up to two orders of magnitude higher than that of the neat matrix, indicating a higher melt elasticity, and better PBAT melt processability. The complex viscosity of neat PBAT is characterized by a linear Newtonian plateau followed at high frequencies by shear thinning. The curves of the biomaterials show instead a non-Newtonian behavior over the whole frequency range, which can be ascribed to the presence of lignin [20,62]. 40R-P had the highest complex viscosity, indicating strong Renol/PBAT interactions. Both an improved interface and a better dispersion would lead to such behavior, in line with the structural, morphological, and thermomechanical analyses. With increasing frequency, the storage modulus and the complex viscosity of 35L-5O-P were lower than that of the neat matrix, showing the plasticizing effect of the ungrafted oil.

Encouraged by the results of batch mixing, we studied the production of biomaterials in a scalable continuous process. Renol (up to 40 wt%) was melt-compounded with PBAT in a single-screw extruder (40 rpm

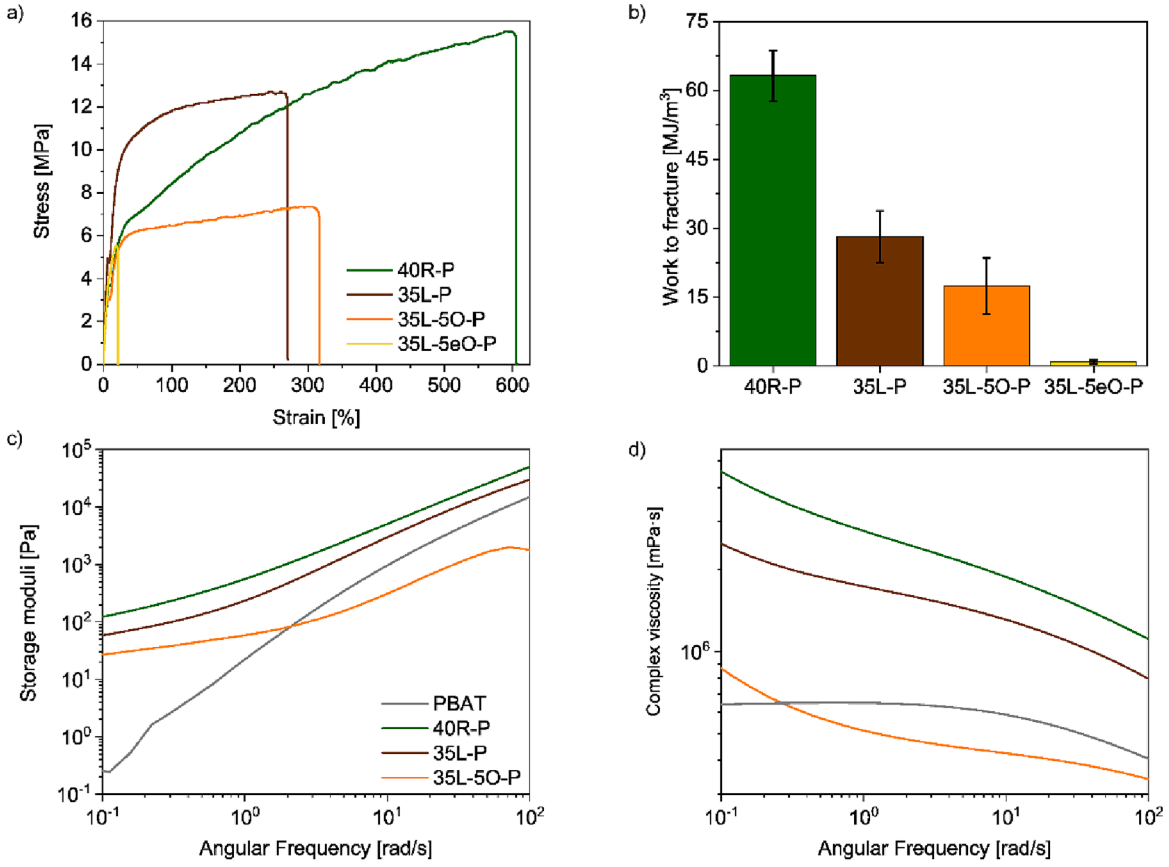

Fig. 7. a) Representative tensile stress–strain curves of 40R-P and its references and b) average work to fracture with standard deviations (areas below the respective tensile curves); c) storage moduli and d) complex viscosity recorded in frequency sweeps by parallel plate dynamic melt rheology at 160 °C.

with a temperature profile of 120–160-140–130 °C). The extruded strands were pelletized, and the pellets were fed for film blowing in the same single-screw extruder (20 rpm and a temperature profile of 120–160-150–120 °C). It was possible to extrude blown films with various thicknesses down to 10 μm, with a blow-up ratio of the bubble to the film die diameter of 6, thanks to the high deformability and melt elasticity of the biomaterials. Fig. 8a shows an image of the film blowing of 40R-P, containing an unprecedented amount of lignin in a blown film. Previous studies [27,59,63,64] have reached a maximum content of 30 wt% solvent-modified lignin [27].

The mechanical properties of the blown films were tested in both the longitudinal and transverse directions (Fig. 8b-e). The stiffness of the biomaterials increased with increasing Renol content, but there was a slight reduction in strength and elongation, retained anyway above 350 %. The blowing process induces anisotropy in the films; the elongation values being greater in the longitudinal direction indicating a preferential polymer chain alignment. The mechanical properties of the biomaterials were compared to two commercial materials used in films for packaging: low-density polyethylene (LDPE) and a grade of biodegradable MaterBi® [65]. Our films showed more than 100 times higher Young's modulus and higher deformability in the longitudinal direction than the commercial materials, but lower tensile strength. From the tensile properties and the easy film blowing standpoint, our biomaterials can compete with commercial packaging films.

Lignin has a good UV-screening ability [66] and this can prevent the detrimental aging of polymers exposed to oxygen, humidity and light. The UV-blocking ability is of interest in outdoor products and packaging, therefore we assessed the transmittance in the UV–vis range of blown films (Fig. 8f). The higher the Renol content, the lower the transmittance, almost zero in the UV range, as schematized in Fig. 8g. To corroborate a potential outdoor application of the films, a water solubility test proved that the biomaterials are not water-soluble, with no

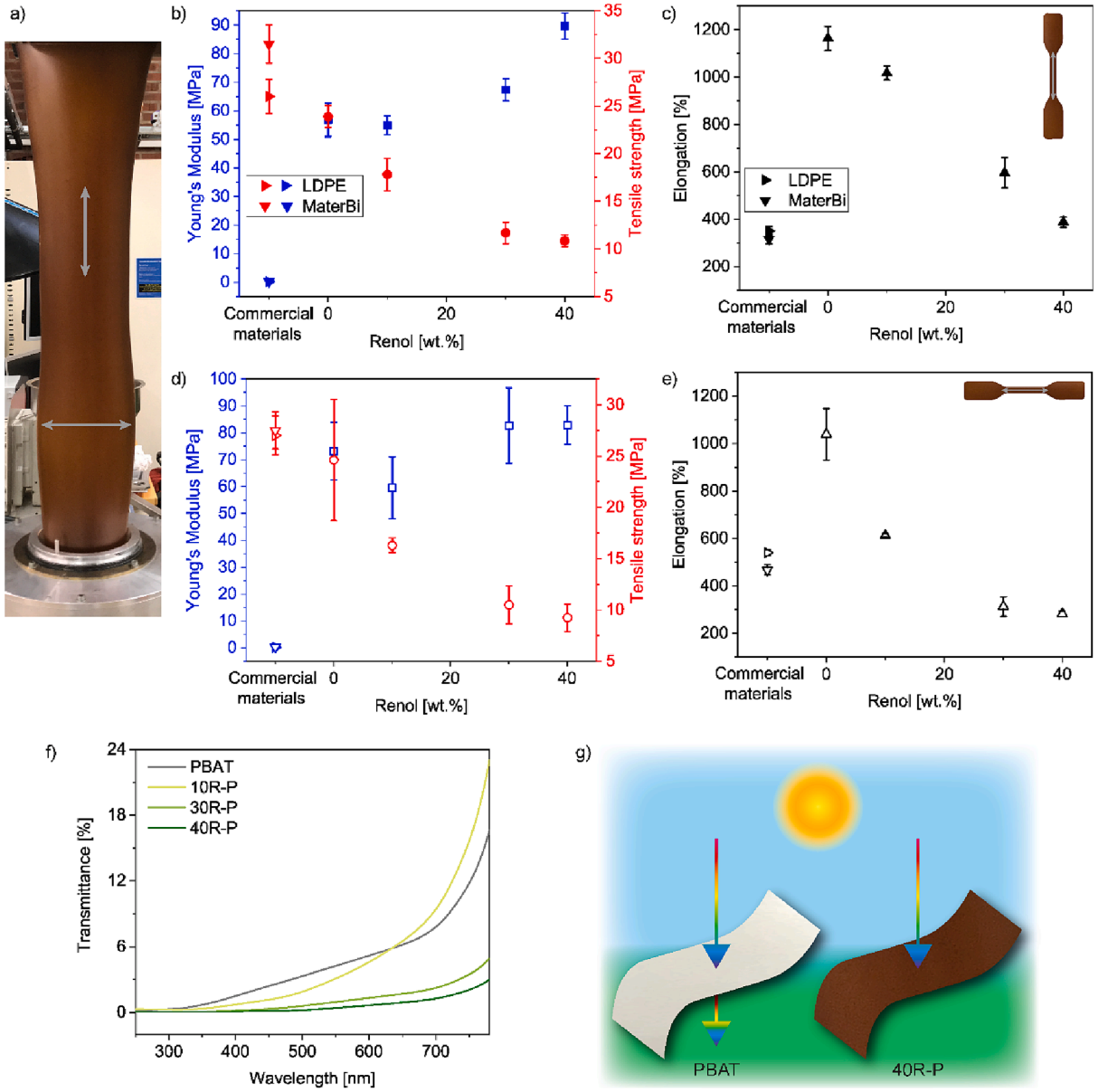

Fig. 8. A) Photograph of 40r-p film blowing. The arrows indicate the longitudinal and transverse directions along which the dumbbell-shaped specimens were cut for the tensile tests. average values with standard deviation in the longitudinal (b, c) and transverse (d, e) directions of: b), d) young's modulus and tensile strength, and c), e) elongation-at-break of the biomaterials compared with film-blown commercial materials,low-density polyethylene (LDPE) and MaterBi®, tested at 50 mm/min by Mistretta et al. [65]. f) Transmittance spectra of blown films recorded in the UV–vis range and g) scheme illustrating the UV-blocking character of the higher lignin content biomaterials compared to PBAT.

significant weight loss over 72 h at 80 °C nor color change of the transparent water indicating no lignin solubilization once incorporated in PBAT (Figure S13).

To assess the end-of-life of the biomaterials, mechanical recycling and disintegration in composting conditions have been studied as i) the most economically advantageous end-of-life option after re-use and ii) the environment-friendly recovery of the raw materials and energy thus closing the loop of the circularity of these biodegradable plastic packaging [67].

After storage for one year under ambient conditions (≈30 RH% and 23 °C), the blown film with 40 wt% Renol has been re-processed under the same conditions in the internal mixer and compression molding (Fig. 9a). Thermal analyses indicate small changes in the thermal properties of the recycled biomaterial (Table S5). In the DSC analysis, the melting temperature and enthalpy shifted to slightly higher values, indicating that the structural rearrangement of the macromolecules had occurred. Thermogravimetric data show a delay of almost 20 °C in the onset of degradation in the recycled material. After aging, the tensile

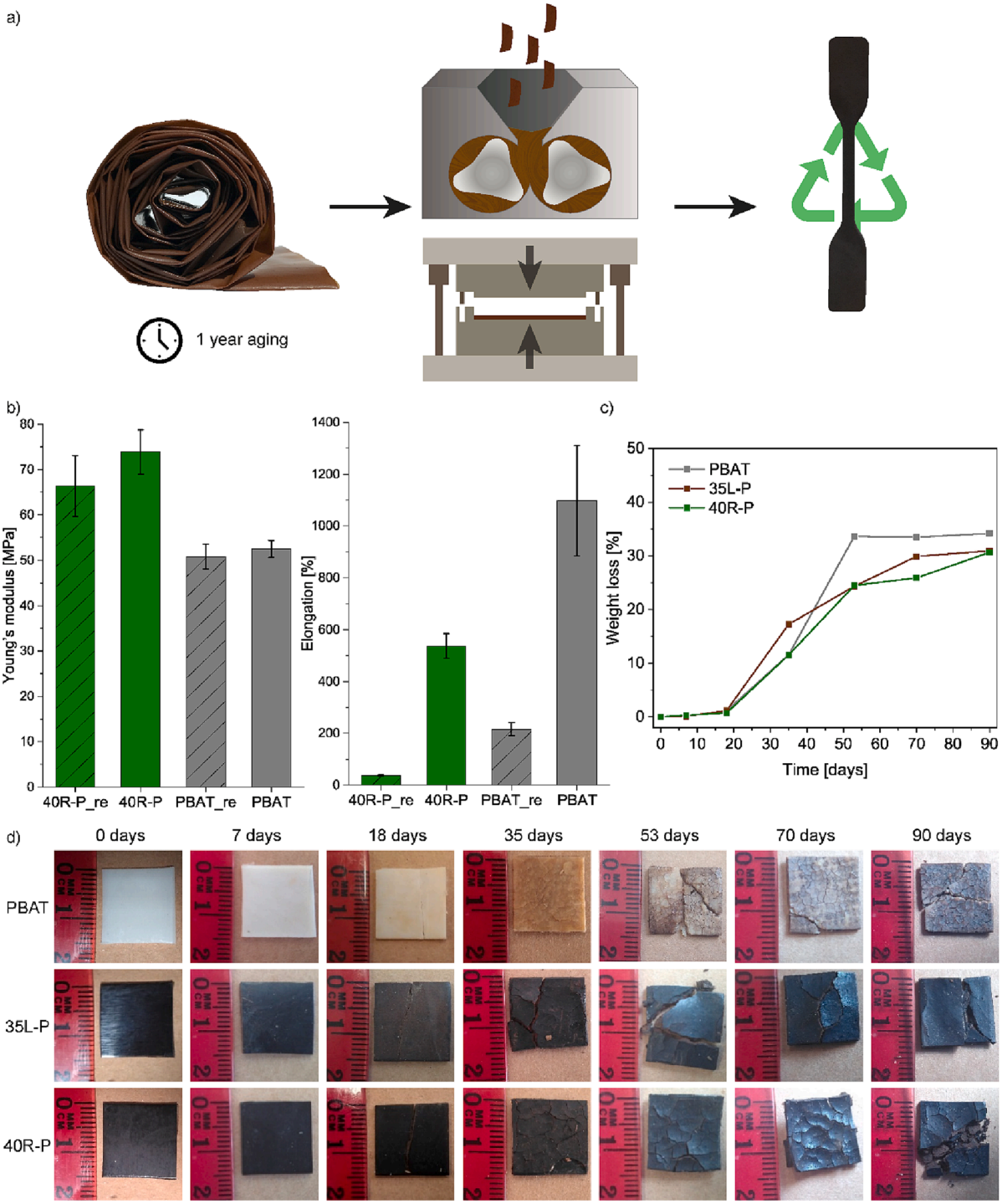

Fig. 9. a) Scheme of the mechanical recycling process, from one-year-aged blown films, melt processing in an internal mixer and compression molding to produce tensile dumbbell-shaped specimens. b) Tensile properties of recycled 40R-P and recycled PBAT compared to their original properties. c) Weight loss as a function of time of neat PBAT and of the biomaterials 35L-P and 40R-P with d) visual appearance at different incubation times under composting conditions.

properties of the recycled film show a similar stiffness but a great embrittlement compared to 40R-P (an elongation at break from 537 % to 37 %) (Fig. 9b). These results suggest that the recycled biomaterials can be used in applications that do not require as extensive deformability, *e. g.* durables, or the need of plasticizers to regain their deformability.

Composting as an end-of-life option has gained considerable attention since the market requires a compostable certification (EN 13432:2000 [68], ASTM D5338 [69] and ISO 20200 [70]) for plastic bags and single-use plastics. In aerobic composting conditions, the biomaterials undergo degradation by microorganisms-controlled biological processes, yielding carbon dioxide, new biomass, and water. In a circular economy perspective, composting allows biomaterials to be reintegrated into a sustainable agricultural system [71]. Therefore, disintegration tests were conducted under composting conditions on a laboratory scale to study the effect of REx and lignin on the fully compostable PBAT [44] (Fig. 9c and 9d, details in SI Ch. 2.1). After 18 days, all the samples show embrittlement (Fig. 9d). Neat PBAT became yellowish while the biomaterials containing 40 wt% Renol and the reference with neat lignin became opaque. The changes in visual aspect have been related to the beginning of the hydrolytic disintegration process [72]. During the hydrolytic process, the water absorption and/or the formation of low molecular weight products lead to a change of the refraction index of the materials. The degradation process of all the samples is characterized by a similar induction time (18 days) driven by the PBAT (Fig. 9c). Up to 35 days, the lignin biomaterial disintegrated faster, most probably due to the lack of adhesion and pull-out (Figure S12) favoring microorganism diffusion in the bulk. For longer times, the rate of neat PBAT disintegration increased, reaching a plateau at 50 days, when the weight loss was around 30 %. The weight losses of the biomaterials after 90 days were similar to that of the PBAT, indicating that the presence of the recalcitrant lignin or Renol did not hinder PBAT disintegration. The fully compostable PBAT (our internal reference) did not completely disintegrate after 90 days, probably because of the thickness of the film (1 mm) and its smooth surface [73,74]. These results demonstrated that the lignin-based materials can indeed disintegrate in compost. To further assess the thickness impact on the degradation rate, test on thinner films (150 μm) are currently under evaluation. The potential toxicity of the degradation products and a deeper understanding of degradation mechanisms are of interest for real applications of these biomaterials and motivate our current investigation.

3.4. Scale-up

The REx production of Renol has been industrially scaled-up with the same Kraft lignin by-product from Stora Enso Sunila mill. The Renol production runs at a rate of 150 kg/h in a Coperion 64 mm twin-screw extruder at the Knivsta (Sweden) unit of Lignin Industries AB. To industrially scale the equivalent biomaterials produced in the laboratory scale, Renol granulates were mixed in different amounts with PBAT at a rate of 300 kg/h. The length of the twin-screw extruded has been adapted to allow the production of Renol or the biomaterials in a single process, adding a side feeder to the extruder for PBAT. The conditions have been therefore optimized to achieve a complete reaction of the eOil with the lignin prior to the feeding of PBAT pellets. The composition with 40 wt% Renol was successfully film-blown to produce films and bags (Fig. 1). The thermal properties of the blend produced on an industrial scale were better than those of the laboratory scale biomaterial (40R-P) (Table 3). The higher onset of thermal degradation and the slightly higher glass transition temperature suggest that a more effective compounding was achieved during extrusion on the industrial scale, where the materials undergo high shear stresses.

Table 3
Thermal properties of laboratory scale 40R-P compared with those of industrial scale (40R-P_industrial): glass transition temperature (T_g), melting temperature (T_m), degree of crystallinity (χ_C), onset of degradation ($T_{5\%}$), temperatures of degradation related to lignin (T_{d1}) and PBAT (T_{d2}) and char residue at 800 °C.

Material	T_g [°C]	T_m [°C]	χ_C [%]	$T_{5\%}$ [°C]	T_{d1} [°C]	T_{d2} [°C]	Char [%]
40R-P_industrial	−13	113	11	303	280	404	22
40R-P	−19	116	13	280	290	402	18

4. Conclusions

Industrial Kraft lignin has been chemically modified with a bio-sourced oil during reactive extrusion, enhancing the lignin's thermoplastic character. The successful grafting of the oil onto lignin has been shown through advanced structural characterization. The modified lignin (Renol) was melt-blended with poly(butylene adipate-co-terephthalate) (PBAT) to produce biomaterials with tunable mechanical properties and renewable content up to 80 wt% lignin. All the processes were designed to avoid the use of any organic solvent or purification step.

Targeting the relevant market of packaging in the need of sustainable alternatives, we achieved to film blow biomaterials with unprecedented lignin-content. All the test indicated better interactions between Renol and PBAT, corroborated by the increase in the content of ester and ether moieties on the modified lignin structure. The morphological analysis confirmed that the reactive process led to a monophasic structure at the observed microscopic level, which enabled film blowing at a high modified lignin content. The mechanical recycling of the biomaterials was validated and their disintegration in composting conditions was comparable to that of the fully compostable PBAT.

This work reports the through the development of biomaterials, starting from a lab scale modification and processing design to the evaluation of the biomaterials' end-of-life, which enabled their industrial scale-up.

Our reliable strategy developed at the laboratory scale has enabled the valorization of unrefined lignin through the production of biomaterials on an industrial scale and common commercial products such as shopping bags. Thanks to the sustainability of the processes and their demonstrated easy scale-up, we believe that this work can serve as a benchmark for the coming generation of circular thermoplastic biomaterials, as demanded by a more responsible society.

Declaration of Competing Interest

The authors declare that they have no known competing financial interests or personal relationships that could have appeared to influence the work reported in this paper.

Data availability

Further data supporting this study are available within the Supporting Information. The Supporting Information contains the following sections: 1 Temperature design for reactive extrusion; 2 Characterization methods; 2.1 Disintegration under composting conditions; 2.2 Thermal analyses; 2.3 Tensile tests; 2.4 Dynamic Mechanical Thermal Analysis (DMTA); 2.5 Morphological analysis; 2.6 Dynamic melt rheology; 2.7 Ultraviolet – visible spectroscopy (UV – vis); 2.8 Attenuated Total Reflection - Fourier-Transform Infrared Spectroscopy (ATR-FTIR); 2.9 Size Exclusion Chromatography (SEC); 2.10 Nuclear magnetic Resonance (NMR); 3 Synthesis of the model compounds; 4 Thermal properties; 5 Tensile properties; 6 Evidence of oil migration; 7 Dynamic thermomechanical properties; 8 Morphological analysis; 9 Water solubility of blown films; 10 Thermal properties of recycled biomaterial. Raw data generated for this work are available on request.

Acknowledgements

This work was supported by the Knut and Alice Wallenberg Biocomposites program [grant number V-2019-0041, Dnr. KAW 2018.0551] and the Wallenberg Wood Science Center (WWSC) 2.0 program. Dr. Nicola Giummarella is acknowledged for the size exclusion chromatography measurements. Dr. J. Anthony Bristow is gratefully acknowledged for the careful linguistic revision.

Appendix A. Supplementary data

Supplementary data to this article can be found online at https://doi.org/10.1016/j.cej.2023.142245.

References

[1] European Bioplastics, Bioplastics market data, (2022). https://www.european-bioplastics.org/market/ (accessed February 21, 2022).
[2] R. Geyer, J.R. Jambeck, K.L. Law, Production, use, and fate of all plastics ever made, Sci. Adv. 3 (2017) e1700782.
[3] J.-G. Rosenboom, R. Langer, G. Traverso, Bioplastics for a circular economy, Nat. Rev. Mater. 72 (7) (2022) 117–137, https://doi.org/10.1038/s41578-021-00407-8.
[4] D. Kai, M.J. Tan, P.L. Chee, Y.K. Chua, Y.L. Yap, X.J. Loh, Towards lignin-based functional materials in a sustainable world, Green Chem. 18 (2016) 1175–1200, https://doi.org/10.1039/C5GC02616D.
[5] T. Saito, R.H. Brown, M.A. Hunt, D.L. Pickel, J.M. Pickel, J.M. Messman, F.S. Baker, M. Keller, A.K. Naskar, Turning renewable resources into value-added polymer: Development of lignin-based thermoplastic, Green Chem. 14 (2012) 3295–3303, https://doi.org/10.1039/c2gc35933b.
[6] T.K. Kirk, R.L. Farrell, Enzymatic "combustion": the microbial degradation of lignin, Annu. Rev. Microbiol. 41 (1987) 465–505, https://doi.org/10.1146/ANNUREV.MI.41.100187.002341.
[7] T. Klotzbücher, K. Kaiser, G. Guggenberger, C. Gatzek, K. Kalbitz, A new conceptual model for the fate of lignin in decomposing plant litter, Ecology. 92 (2011) 1052–1062, https://doi.org/10.1890/10-1307.1.
[8] L.P. Christopher, Integrated Forest Biorefineries: Current State and Development Potential, in: L. Christopher (Ed.), Integrated Forest Biorefineries, The Royal Society of Chemistry, 2012, pp. 1–66.
[9] Y.Y. Wang, X. Meng, Y. Pu, A.J. Ragauskas, Recent advances in the application of functionalized lignin in value-added polymeric materials, Polymers. 12 (2020) 1–24, https://doi.org/10.3390/polym12102277.
[10] S.-J. Zhou, H.-M. Wang, S.-J. Xiong, J.-M. Sun, Y.-Y. Wang, S. Yu, Z. Sun, J.-L. Wen, T.-Q. Yuan, Technical Lignin Valorization in Biodegradable Polyester-Based Plastics (BPPs), ACS Sustain, Chem. Eng. (2021) 12017–12042, https://doi.org/10.1021/acssuschemeng.1c03705.
[11] X. Zhou, T. He, Y. Jiang, S. Chang, Y. Yu, X. Fang, Y. Zhang, A Novel Network-Structured Compatibilizer for Improving the Interfacial Behavior of PBS/Lignin, ACS Sustain, Chem. Eng. (2021) 8592–8602, https://doi.org/10.1021/acssuschemeng.1c01962.
[12] S. Luo, J. Cao, A.G. McDonald, Interfacial Improvements in a Green Biopolymer Alloy of Poly(3-hydroxybutyrate-co-3-hydroxyvalerate) and Lignin via in Situ Reactive Extrusion, ACS Sustain. Chem. Eng. 4 (2016) 3465–3476, https://doi.org/10.1021/acssuschemeng.6b00495.
[13] V.R. Romhányi, D. Dávid Kun, B.P. Pukánszky, Correlations among Miscibility, Structure, and Properties in Thermoplastic Polymer/Lignin Blends, (2018) 14323−14331. 10.1021/acssuschemeng.8b02989.
[14] Y. Tang, M. Jean, S. Pourebrahimi, D. Rodrigue, Z. Ye, Influence of lignin structure change during extrusion on properties and recycling of lignin-polyethylene thermoplastic composites, Can. J. Chem. Eng. 99 (2021) S27–S38, https://doi.org/10.1002/CJCE.23960.
[15] D. Kun, B. Pukánszky, Polymer/lignin blends: Interactions, properties, applications, Eur. Polym. J. 93 (2017) 618–641, https://doi.org/10.1016/j.eurpolymj.2017.04.035.
[16] R. Chen, M.A. Abdelwahab, M. Misra, A.K. Mohanty, Biobased Ternary Blends of Lignin, Poly(Lactic Acid), and Poly(Butylene Adipate-co-Terephthalate): The Effect of Lignin Heterogeneity on Blend Morphology and Compatibility, J. Polym. Environ. 22 (2014) 439–448, https://doi.org/10.1007/s10924-014-0704-5.
[17] C. Wang, S.S. Kelley, R.A. Venditti, Lignin-Based Thermoplastic Materials, ChemSusChem. 9 (2016) 770–783, https://doi.org/10.1002/cssc.201501531.
[18] S. Bhagia, K. Bornani, R. Agarwal, A. Satlewal, J. Ďurkovič, R. Lagaňa, M. Bhagia, C.G. Yoo, X. Zhao, V. Kunc, Y. Pu, S. Ozcan, A.J. Ragauskas, Critical review of FDM 3D printing of PLA biocomposites filled with biomass resources, characterization, biodegradability, upcycling and opportunities for biorefineries, Appl. Mater. Today. 24 (2021), 101078, https://doi.org/10.1016/J.APMT.2021.101078.
[19] F. Chen, H. Dai, X. Dong, J. Yang, M. Zhong, Physical properties of lignin-based polypropylene blends, Polym. Compos. 32 (2011) 1019–1025, https://doi.org/10.1002/PC.21087.
[20] X. Guo, X. Junna, M.P. Wolcott, J. Zhang, Mechanochemical Oleation of Lignin Through Ball Milling and Properties of its Blends with PLA, ChemistrySelect. 1 (2016) 3449–3454, https://doi.org/10.1002/SLCT.201600633.
[21] J.F. Kadla, S. Kubo, Miscibility and Hydrogen Bonding in Blends of Poly(ethylene oxide) and Kraft Lignin, Macromolecules. 36 (2003) 7803–7811, https://doi.org/10.1021/MA0348371.
[22] H.M. Wang, B. Wang, T.Q. Yuan, L. Zheng, Q. Shi, S.F. Wang, G.Y. Song, R.C. Sun, Tunable, UV-shielding and biodegradable composites based on well-characterized lignins and poly(butylene adipate-co-terephthalate), Green Chem. 22 (2020) 8623–8632, https://doi.org/10.1039/D0GC03284K.
[23] Q. Xing, D. Ruch, P. Dubois, L. Wu, W.J. Wang, Biodegradable and High-Performance Poly(butylene adipate-co-terephthalate)-Lignin UV-Blocking Films, ACS Sustain. Chem. Eng. 5 (2017) 10342–10351, https://doi.org/10.1021/acssuschemeng.7b02370.
[24] Y. Liu, S. Liu, Z. Liu, Y. Lei, S. Jiang, K. Zhang, W. Yan, J. Qin, M. He, S. Qin, J. Yu, Enhanced mechanical and biodegradable properties of PBAT/lignin composites via silane grafting and reactive extrusion, Compos. Part B Eng. 220 (2021), 108980, https://doi.org/10.1016/J.COMPOSITESB.2021.108980.
[25] Q. Xing, P. Buono, D. Ruch, P. Dubois, L. Wu, W.-J. Wang, Biodegradable UV-Blocking Films through Core-Shell Lignin–Melanin Nanoparticles in Poly(butylene adipate- co -terephthalate), ACS Sustain. Chem. Eng. 7 (2019) 4147–4157, https://doi.org/10.1021/acssuschemeng.8b05755.
[26] X. Yang, S. Zhong, Properties of maleic anhydride-modified lignin nanoparticles/polybutylene adipate-co-terephthalate composites, J. Appl. Polym. Sci. 137 (2020) 1–8, https://doi.org/10.1002/app.49025.
[27] W.G. Glasser, R. Loos, B. Cox, H. Cao, Melt-blown compostable polyester films with lignin, Tappi J. 16 (2017) 111–121, https://doi.org/10.32964/tj16.3.111.
[28] G. Gellerstedt, Softwood kraft lignin: Raw material for the future, Ind. Crops Prod. 77 (2015) 845–854, https://doi.org/10.1016/J.INDCROP.2015.09.040.
[29] A. Nagardeolekar, M. Ovadias, P. Dongre, B. Bujanovic, Prospects and Challenges of Using Lignin for Thermoplastic Materials, in: C.G. Yoo, A. Ragauskas (Eds.), Lignin Util. Strateg. From Process. to Appl., American Chemical Society, 2021: pp. 231–271. 10.1021/bk-2021-1377.ch010.
[30] J.M. Raquez, R. Narayan, P. Dubois, Recent advances in reactive extrusion processing of biodegradable polymer-based compositions, Macromol. Mater. Eng. 293 (2008) 447–470, https://doi.org/10.1002/mame.200700395.
[31] S. Spinella, M. Ganesh, G. Lo Re, S. Zhang, J.M. Raquez, P. Dubois, R.A. Gross, Enzymatic reactive extrusion: moving towards continuous enzyme-catalysed polyester polymerisation and processing, Green Chem. 17 (2015) 4146–4150, https://doi.org/10.1039/c5gc00992h.
[32] R. Mani, M. Bhattacharya, J. Tang, Functionalization of Polyesters with Maleic Anhydride by Reactive Extrusion, J Polym Sci A Polym Chem. 37 (1999) 1693–1702, https://doi.org/10.1002/(SICI)1099-0518(19990601)37:11.
[33] C.-W. Park, W.-J. Youe, S.-J. Kim, S.-Y. Han, J.-S. Park, E.-A. Lee, G.-J. Kwon, Y.-S. Kim, N.-H. Kim, S.-H. Lee, Effect of Lignin Plasticization on Physico-Mechanical Properties of Lignin/Poly(Lactic Acid) Composites, Polymers. 11 (2019) 2089, https://doi.org/10.3390/polym11122089.
[34] S. Rojas-Lema, J. Ivorra-Martinez, D. Lascano, D. Garcia-Garcia, R. Balart, Improved Performance of Environmentally Friendly Blends of Biobased Polyethylene and Kraft Lignin Compatibilized by Reactive Extrusion with Dicumyl Peroxide, Macromol. Mater. Eng. 306 (2021) 2100196, https://doi.org/10.1002/MAME.202100196.
[35] N. Kanbargi, M. Goswami, L. Collins, L.T. Kearney, C.C. Bowland, K. Kim, K. Rajan, N. Labbe, A.K. Naskar, Synthesis of High-Performance Lignin-Based Inverse Thermoplastic Vulcanizates with Tailored Morphology and Properties, ACS Appl. Polym. Mater. (2021) 2911–2920, https://doi.org/10.1021/acsapm.0c01387.
[36] W. Yang, F. Dominici, E. Fortunati, J.M. Kenny, D. Puglia, Effect of lignin nanoparticles and masterbatch procedures on the final properties of glycidyl methacrylate-g-poly (lactic acid) films before and after accelerated UV weathering, Ind. Crops Prod. 77 (2015) 833–844, https://doi.org/10.1016/J.INDCROP.2015.09.057.
[37] S.J. Xiong, B. Pang, S.J. Zhou, M.K. Li, S. Yang, Y.Y. Wang, Q. Shi, S.F. Wang, T. Q. Yuan, R.C. Sun, Economically Competitive Biodegradable PBAT/Lignin Composites: Effect of Lignin Methylation and Compatibilizer, ACS Sustain. Chem. Eng. 8 (2020) 5338–5346, https://doi.org/10.1021/acssuschemeng.0c00789.
[38] J.H. Bridson, D.J. Van De Pas, A. Fernyhough, Succinylation of three different lignins by reactive extrusion, J. Appl. Polym. Sci. 128 (2013) 4355–4360, https://doi.org/10.1002/APP.38664.
[39] R. Milotskyi, L. Szabó, K. Takahashi, C. Bliard, Chemical Modification of Plasticized Lignins Using Reactive Extrusion, Front. Chem. 7 (2019), https://doi.org/10.3389/fchem.2019.00633.
[40] W. Farhat, R. Venditti, N. Mignard, M. Taha, F. Becquart, A. Ayoub, Polysaccharides and lignin based hydrogels with potential pharmaceutical use as a drug delivery system produced by a reactive extrusion process, Int. J. Biol. Macromol. 104 (2017) 564–575, https://doi.org/10.1016/J.IJBIOMAC.2017.06.037.
[41] S. Li, W. Xie, M. Wilt, J.A. Willoughby, O.J. Rojas, Thermally Stable and Tough Coatings and Films Using Vinyl Silylated Lignin, ACS Sustain. Chem. Eng. 6 (2018) 1988–1998, https://doi.org/10.1021/acssuschemeng.7b03387.
[42] M. Zhang, G.M. Biesold, W. Choi, J. Yu, Y. Deng, C. Silvestre, Z. Lin, Recent advances in polymers and polymer composites for food packaging, Mater. Today. 53 (2022) 134–161, https://doi.org/10.1016/J.MATTOD.2022.01.022.
[43] Y.X. Weng, Y.J. Jin, Q.Y. Meng, L. Wang, M. Zhang, Y.Z. Wang, Biodegradation behavior of poly(butylene adipate-co-terephthalate) (PBAT), poly(lactic acid) (PLA), and their blend under soil conditions, Polym. Test. 32 (2013) 918–926, https://doi.org/10.1016/J.POLYMERTESTING.2013.05.001.
[44] J. Jian, Z. Xiangbin, H. Xianbo, An overview on synthesis, properties and applications of poly(butylene-adipate-co-terephthalate)–PBAT, Adv. Ind. Eng. Polym. Res. 3 (2020) 19–26, https://doi.org/10.1016/J.AIEPR.2020.01.001.

[45] European Union, Turning the tide on single-use plastics - Publications Office of the EU, (2021). https://op.europa.eu/en/publication-detail/-/publication/49fc9754-ca5a-11eb-84ce-01aa75ed71a1 (accessed August 16, 2022).
[46] European Commission, Bio-based, biodegradable and compostable plastics, (2022). https://environment.ec.europa.eu/topics/plastics/bio-based-biodegradable-and-compostable-plastics_en (accessed August 16, 2022).
[47] O. Gordobil, R. Moriana, L. Zhang, J. Labidi, O. Sevastyanova, Assesment of technical lignins for uses in biofuels and biomaterials: Structure-related properties, proximate analysis and chemical modification, Ind. Crops Prod. 83 (2016) 155–165, https://doi.org/10.1016/j.indcrop.2015.12.048.
[48] B.R. Moser, S.C. Cermak, K.M. Doll, J.A. Kenar, B.K. Sharma, A review of fatty epoxide ring opening reactions: Chemistry, recent advances, and applications, JAOCS, J. Am. Oil Chem. Soc. 99 (2022) 801–842, https://doi.org/10.1002/AOCS.12623.
[49] C. Gioia, G. Lo Re, M. Lawoko, L. Berglund, Tunable Thermosetting Epoxies Based on Fractionated and Well-Characterized Lignins, J. Am. Chem. Soc. 140 (2018) 4054–4061, https://doi.org/10.1021/jacs.7b13620.
[50] D.S. Argyropoulos, Quantitative phosphorus-31 nmr analysis of lignins, a new tool for the lignin chemist, J. Wood Chem. Technol. 14 (1994) 45–63, https://doi.org/10.1080/02773819408003085.
[51] N. Giummarella, P.A. Lindén, D. Areskogh, M. Lawoko, Fractional Profiling of Kraft Lignin Structure: Unravelling Insights on Lignin Reaction Mechanisms, ACS Sustain. Chem. Eng. 8 (2020) 1112–1120, https://doi.org/10.1021/acssuschemeng.9b06027.
[52] N. Giummarella, I.V. Pylypchuk, O. Sevastyanova, M. Lawoko, New Structures in Eucalyptus Kraft Lignin with Complex Mechanistic Implications, ACS Sustain. Chem. Eng. 8 (2020) 10983–10994, https://doi.org/10.1021/acssuschemeng.0c03776.
[53] C. Crestini, H. Lange, M. Sette, D.S. Argyropoulos, On the structure of softwood kraft lignin, Green Chem. 19 (2017) 4104–4121, https://doi.org/10.1039/C7GC01812F.
[54] C.S. Lancefield, H.J. Wienk, R. Boelens, B.M. Weckhuysen, P.C.A. Bruijnincx, Identification of a diagnostic structural motif reveals a new reaction intermediate and condensation pathway in kraft lignin formation, Chem. Sci. 9 (2018) 6348–6360, https://doi.org/10.1039/C8SC02000K.
[55] C. Zhao, Z. Hu, L. Shi, C. Wang, F. Yue, S. Li, H. Zhang, F. Lu, Profiling of the formation of lignin-derived monomers and dimers from Eucalyptus alkali lignin, Green Chem. 22 (2020) 7366–7375, https://doi.org/10.1039/D0GC01658F.
[56] E. Oliva, D. Mathiron, S. Rigaud, E. Monflier, E. Sevin, H. Bricout, S. Tilloy, F. Gosselet, L. Fenart, V. Bonnet, S. Pilard, F. Djedaini-Pilard, New Lipidyl-Cyclodextrins Obtained by Ring Opening of Methyl Oleate Epoxide Using Ball Milling, Biomolecules. 10 (2020) 339, https://doi.org/10.3390/BIOM10020339.
[57] D. Łukawski, W. Grześkowiak, A. Lekawa-Raus, M. Widelicka, F. Lisiecki, A. Dudkowiak, Flame retardant effect of lignin/carbon nanotubes/potassium carbonate composite coatings on cotton roving, Cellulose. 27 (2020) 7271–7281, https://doi.org/10.1007/s10570-020-03270-y.
[58] M.A. Abdelwahab, S. Taylor, M. Misra, A.K. Mohanty, Thermo-mechanical characterization of bioblends from polylactide and poly(butylene adipate-co-terephthalate) and lignin, Macromol. Mater. Eng. 300 (2015) 299–311, https://doi.org/10.1002/mame.201400241.
[59] X. Gu, J. Hou, S. Ai, Effect of silane modified nano-SiO2 on the mechanical properties and compatibility of PBAT/lignin composite films, J. Appl. Polym. Sci. 139 (2022), https://doi.org/10.1002/app.52051.
[60] H. Kargarzadeh, A. Galeski, A. Pawlak, PBAT green composites: Effects of kraft lignin particles on the morphological, thermal, crystalline, macro and micromechanical properties, Polymer (Guildf). 203 (2020), 122748, https://doi.org/10.1016/j.polymer.2020.122748.
[61] M. Li, Y. Jia, X. Shen, T. Shen, Z. Tan, W. Zhuang, G. Zhao, C. Zhu, H. Ying, Investigation into lignin modified PBAT/thermoplastic starch composites: Thermal, mechanical, rheological and water absorption properties, Ind. Crops Prod. 171 (2021), https://doi.org/10.1016/J.INDCROP.2021.113916.
[62] A. Ghosh, K. Kim, K. Rajan, C.C. Bowland, R.N. Gurram, R.W. Montgomery, A. Manesh, N. Labbé, A.K. Naskar, Butanol-based organosolv lignin and reactive modification of poly(ethylene-glycidyl methacrylate), Ind. Eng. Chem. Res. 58 (2019) 20300–20308, https://doi.org/10.1021/acs.iecr.9b04071.
[63] L.P. Amaro, H. Chen, A. Barghini, A. Corti, E. Chiellini, High performance compostable biocomposites based on bacterial polyesters suitable for injection molding and blow extrusion, Chem. Biochem. Eng. Q. 29 (2015) 261–274. 10.15255/CABEQ.2014.2259.
[64] J. Huang, S. Fu, L. Gan, eds., Lignin-Modified Thermoplastic Materials, in: Lignin Chem. Appl., Elsevier, 2019: pp. 135–161. 10.1016/B978-0-12-813941-7.00005-9.
[65] M.C. Mistretta, L. Botta, R. Arrigo, F. Leto, G. Malucelli, F.P. La Mantia, Bionanocomposite blown films: Insights on the rheological and mechanical behavior, Polymers 13 (2021), https://doi.org/10.3390/polym13071167.
[66] Q. Xia, C. Chen, Y. Yao, J. Li, S. He, Y. Zhou, T. Li, X. Pan, Y. Yao, L. Hu, A strong, biodegradable and recyclable lignocellulosic bioplastic, Nat. Sustain. (2021), https://doi.org/10.1038/s41893-021-00702-w.
[67] European Commission, Waste Framework Directive, (2022). https://environment.ec.europa.eu/topics/waste-and-recycling/waste-framework-directive_en (accessed August 18, 2022).
[68] British Standards Institution, EN 13432:2000 - Packaging. Requirements for Packaging Recoverable through Composting and Biodegradation. Test Scheme and Evaluation Criteria for the Final Acceptance of Packaging, (2000) 1–26.
[69] ASTM International, ASTM D5338–15(2021) standard test method for determining aerobic biodegradation of plastic materials under controlled composting conditions, Incorporating Thermophilic Temperatures (2021), https://doi.org/10.1520/D5338-15R21.
[70] ISO, ISO 20200:2015(en), Plastics — Determination of the degree of disintegration of plastic materials under simulated composting conditions in a laboratory-scale test, (2015).
[71] F. Ruggero, R.C.A. Onderwater, E. Carretti, S. Roosa, S. Benali, J.M. Raquez, R. Gori, C. Lubello, R. Wattiez, Degradation of film and rigid bioplastics during the thermophilic phase and the maturation phase of simulated composting, J. Polym. Environ. 29 (2021) 3015–3028, https://doi.org/10.1007/S10924-021-02098-2/FIGURES/7.
[72] V. Sessini, M.P. Arrieta, J.M. Raquez, P. Dubois, J.M. Kenny, L. Peponi, Thermal and composting degradation of EVA/Thermoplastic starch blends and their nanocomposites, Polym. Degrad. Stab. 159 (2019) 184–198, https://doi.org/10.1016/J.POLYMDEGRADSTAB.2018.11.025.
[73] T. Kijchavengkul, R. Auras, M. Rubino, M. Ngouajio, R.T. Fernandez, Assessment of aliphatic-aromatic copolyester biodegradable mulch films. Part I: Field study, Chemosphere 71 (2008) 942–953, https://doi.org/10.1016/j.chemosphere.2007.10.074.
[74] N. Nomadolo, O.E. Dada, A. Swanepoel, T. Mokhena, S. Muniyasamy, A Comparative Study on the Aerobic Biodegradation of the Biopolymer Blends of Poly(butylene succinate), Poly(butylene adipate terephthalate) and Poly(lactic acid), Polymers. 14 (2022) 1894, https://doi.org/10.3390/polym14091894.